

Observation of spontaneous combustion of hydrogen and oxygen in microbubbles

A. V. Postnikov, I. V. Uvarov, A. V. Prokaznikov, and V. B. Svetovoy

Citation: [Applied Physics Letters](#) **108**, 121604 (2016); doi: 10.1063/1.4944780

View online: <http://dx.doi.org/10.1063/1.4944780>

View Table of Contents: <http://scitation.aip.org/content/aip/journal/apl/108/12?ver=pdfcov>

Published by the [AIP Publishing](#)

Articles you may be interested in

[Forces acting on a particle in a concentration gradient under an externally applied oscillating electric field](#)

Appl. Phys. Lett. **105**, 094105 (2014); 10.1063/1.4894731

[Insight into instabilities in burning droplets](#)

Phys. Fluids **26**, 032101 (2014); 10.1063/1.4866866

[Field nano-localization of gas bubble production from water electrolysis](#)

Appl. Phys. Lett. **103**, 223106 (2013); 10.1063/1.4836095

[Colloidal electroconvection in a thin horizontal cell. III. Interfacial and transient patterns on electrodes](#)

J. Chem. Phys. **137**, 014504 (2012); 10.1063/1.4730752

[Cavitation-induced ignition of cryogenic hydrogen-oxygen fluids](#)

Appl. Phys. Lett. **98**, 134102 (2011); 10.1063/1.3571445



NEW Special Topic Sections

NOW ONLINE
Lithium Niobate Properties and Applications:
Reviews of Emerging Trends

AIP | Applied Physics
Reviews

Observation of spontaneous combustion of hydrogen and oxygen in microbubbles

A. V. Postnikov,¹ I. V. Uvarov,¹ A. V. Prokaznikov,¹ and V. B. Svetovoy^{1,2,a)}

¹Yaroslavl Branch of the Institute of Physics and Technology, Russian Academy of Sciences, 150007 Yaroslavl, Russia

²MESA⁺ Institute for Nanotechnology, University of Twente, P.O. Box 217, 7500 AE Enschede, The Netherlands

(Received 5 December 2015; accepted 13 March 2016; published online 23 March 2016)

Experimental evidence is presented that combustion can ignite at room temperature spontaneously inside microbubbles filled with mixture of hydrogen and oxygen. We perform water electrolysis in a closed microchamber by voltage pulses of alternating polarity at repetition frequencies ≥ 100 kHz to pump the gases rapidly into the electrolyte and produce extreme supersaturation with both gases. After a delay of 300 – 600 μ s, we observe stroboscopically microbubbles of 5 – 20 μ m in diameter that appear in between the electrodes for several microseconds. Each event is accompanied by a pressure jump of 0.1 – 1 bar that is measured interferometrically. The pressure jumps are attributed to combustion of the gases in the microbubbles. © 2016 AIP Publishing LLC. [<http://dx.doi.org/10.1063/1.4944780>]

It is well known that combustion reactions quench in a small volume due to fast heat escape via the volume boundaries.^{1,2} Surprisingly, spontaneous reaction between H₂ and O₂ gases was recently observed in nanobubbles (NBs) that were produced in microsystems by alternating polarity electrolysis of water.^{3–5} However, direct optical observation of the combustion was not possible because of the small size of the bubbles and their short lifetime.

In this paper, we describe a different regime of the alternating polarity electrolysis, in which short-lived microbubbles (MBs) containing a stoichiometric mixture of hydrogen and oxygen are formed. These MBs can be observed optically, exist about 3 μ s, and their short appearance is accompanied by significant pressure jumps in the closed chamber. We will argue that only the combustion reaction between the gases has the appropriate energy and time scales to explain the observed phenomena.

The microdevices (see Fig. 1) were fabricated on Si wafers covered with a layer of silicon nitride of 530 nm thick. Platinum electrodes were deposited on top of this layer. The chamber and filling channels were isotropically etched in borofloat glass and then anodically bonded to the Si substrate. The nominal dimensions of the chamber were $5 \times 100 \times 100 \mu\text{m}^3$. A flexible membrane was formed below the chamber area by etching through the Si wafer from the back side and releasing the layer of silicon nitride. Details of the design and fabrication were reported earlier.⁵ The chamber was filled with a 1M solution of Na₂SO₄ in deionized water, and the in/outlet openings of the long filling channels were sealed afterwards.

To generate both hydrogen and oxygen above each electrode, square voltage pulses of alternating sign were applied between them at frequencies $f \geq 100$ kHz. The chamber was observed with a homemade stroboscope⁶ (exposure time

$\tau_{str} = 7 - 10 \mu\text{s}$, wavelength $\lambda \approx 530$ nm, and space resolution $\sim 1 \mu\text{m}$). Gas production in the chamber resulted in a pressure rise. This pressure was recorded by measuring the deflection of the membrane with a vibrometer (Polytec MSA-400). The laser beam ($\lambda = 633$ nm, size 1.5 μm) was focused on an opaque spot on the back of the membrane to prevent possible scattering by bubbles formed in the chamber. The membrane deflection d was calibrated by applying a static gas pressure, resulting in $\Delta P = 2.03d + 0.27d^3$,⁵ where ΔP is the overpressure in bars and d is in μm . Simultaneously, the electrical current was measured on another channel of the vibrometer, providing information on both the Faraday current⁴ and the temperature near the electrodes.⁵

Figures 2(a) and 2(b) show stroboscopic snapshots of the chamber at times $t = 400 \mu\text{s}$ and $t = 800 \mu\text{s}$ after turning on the pulses. The process was driven at $f = 100$ kHz with a voltage amplitude of $U = 8$ V. At $t = 400 \mu\text{s}$, a small number of bubbles is visible above the electrodes, which are sharp and long-lived. Most of the bubbles in this case are NBs, which are not visible optically since they do not scatter light. This regime was described in detail earlier.⁵ The image in (b) differs in two aspects. First, one can see some contrast in between the electrodes, resembling bubbles with diameters 5 – 10 μm . They appear out of focus due to motion blur, which implies that they exist less than the exposure time,

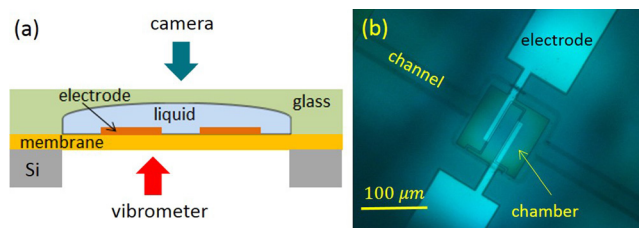


FIG. 1. (a) Schematic representation of the chamber. (b) Top view of the device. The chamber, filling channels, and electrodes are shown.

^{a)}Author to whom correspondence should be addressed. Electronic mail: v.svetovoy@utwente.nl

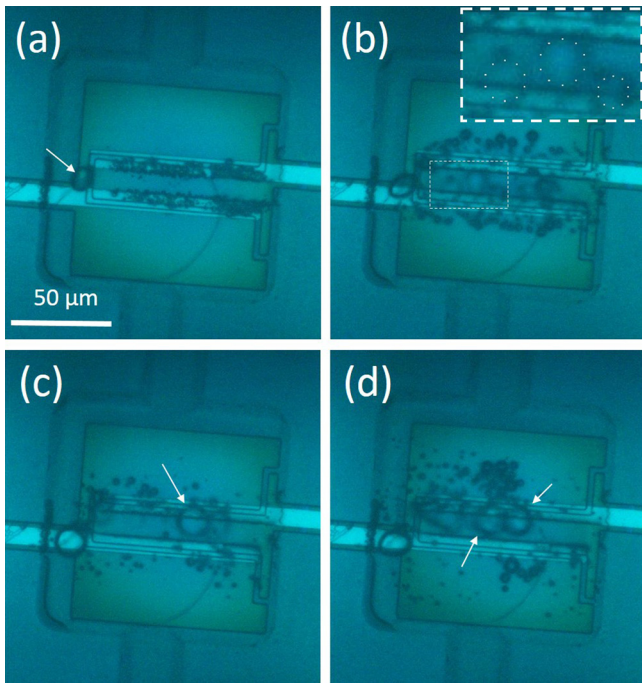


FIG. 2. Snapshots made with the stroboscope at different conditions. Images (a) and (b) show the chamber at times $t = 400 \mu\text{s}$ and $800 \mu\text{s}$, respectively, driven by alternating polarity pulses at $f = 100 \text{ kHz}$. The arrow in (a) indicates a pinned bubble. Short-lived MBs are visible in between the electrodes in (b) as “out of focus” large bubbles. The bubble boundaries are indicated by dots. Images (c) and (d) were made at $t = 1200 \mu\text{s}$ and $3200 \mu\text{s}$ for driving frequency $f = 200 \text{ kHz}$. Some of the short-lived bubbles are indicated by the arrows.

$10 \mu\text{s}$. For better visibility, the dashed box is zoomed in the inset, and three bubbles in view are approximated by circles of 10, 9, and $7 \mu\text{m}$ in diameter. Second, during the process, the long-lived bubbles, which are in focus and smaller in size, were pushed away from the electrodes. Images (c) and (d) were made at higher driving frequency $f = 200 \text{ kHz}$ and at later moments of time $t = 1200 \mu\text{s}$ and $t = 3200 \mu\text{s}$, respectively. The arrows in these images indicate some of the short-lived microbubbles with the size around $14 \mu\text{m}$. These bubbles are larger than at $f = 100 \text{ kHz}$, appear after longer delay time, and the forces pushing the long-lived bubbles are stronger.

Membrane deflection measured with the vibrometer was transformed to the overpressure ΔP in the chamber with the calibration curve. Figure 3(a) shows the overpressure in response to the driving pulses with $U = 9 \text{ V}$ and $f = 150 \text{ kHz}$. First, ΔP increases with time up to the moment $t \approx 550 \mu\text{s}$. During this time, very few gas is visible in the chamber similar to that in Fig. 2(a). At a later time, the pressure starts to fluctuate and the situation in the chamber corresponds with Fig. 2(b). A typical pressure jump is shown in Fig. 3(b). Its magnitude is $\delta P \approx 0.2 \text{ bar}$, and the width is $\delta t \approx 3 \mu\text{s}$. The average amplitude of the jumps increases with the driving frequency. At frequencies below 100 kHz , the pressure does not fluctuate so strongly and the short-lived MBs are not observed. The pressure fluctuations correlate in time with the appearance of the short-lived microbubbles observed by the stroboscope.

The Faraday current is shown in Fig. 3(c). It was extracted from the total current, which contains also the

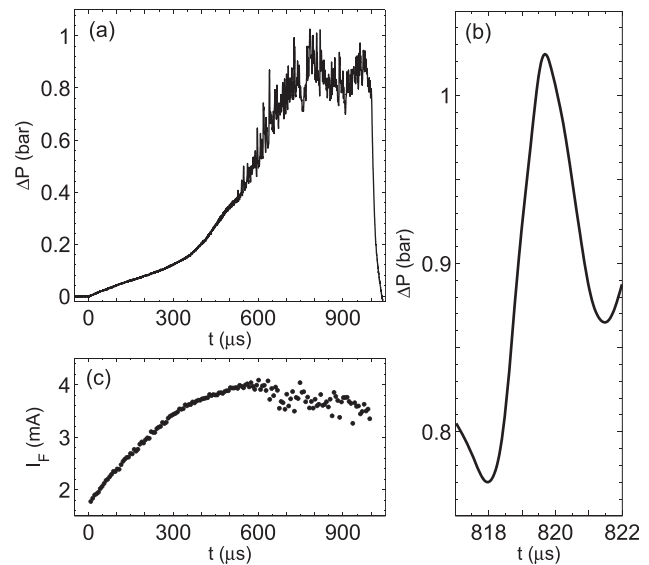


FIG. 3. (a) Overpressure as a function of time for the process driven at $U = 9 \text{ V}$ and $f = 150 \text{ kHz}$. (b) A zoomed pressure peak from panel (a) represents a typical pressure jump. (c) The Faraday current extracted from the total current (one point per period).

reactive component. Each current pulse (half of the period) was fitted by the function $I(t) = I_F + I_1 e^{-t/\tau}$, in which the second term is responsible for the charging-discharging of the interface and τ is the relaxation time. This procedure gives good description of the current at different conditions.^{4,5} In the beginning the Faraday current monotonously increases with time due to gradual temperature increase that happens as the result of Joule heat and the heat produced by the reaction in NBs.⁵ Later, when the short-lived MBs start to appear in between the electrodes, the current develops a significant fluctuating component. These fluctuations can be expected because MBs comparable in size with the distance between the electrodes disrupt the current flow in the electrolyte.

We conclude that the pressure jumps and the current fluctuations are induced by the short-lived bubbles observed optically. The bubbles are not a result of a boiling. The temperature in the chamber is estimated as $70 \text{ }^\circ\text{C}$ (the temperature coefficient of the Faraday current is 0.024 K^{-1} (Ref. 5)) while the boiling point in the chamber at pressure $P \approx 1.8 \text{ bar}$ is around $117 \text{ }^\circ\text{C}$.

The total number of gas molecules N produced in the system can be estimated from the current as $N = (3/4) \int dt I_F(t)/e \approx 1.6 \times 10^{13}$, where e is the electron charge. After relaxation of the pressure, all of this gas has to fill a volume equal to $13V_{ch}$, where $V_{ch} = 5 \times 10^4 \mu\text{m}^3$ is the volume of the chamber. Such large amounts of gas were not observed in the alternating polarity electrolysis at high frequencies. However, all of this gas shows up if stoichiometry of gas production above the same electrode is broken,³ for example, if single polarity pulses are applied to the electrode or if duty cycle of alternating polarity pulses is not equal to 0.5. Disappearance of the gas produced electrochemically was explained by the reaction of gases in stoichiometric NBs.^{3,5} Although the mechanism of the reaction is unclear, there are very few doubts that the reaction happens because a huge amount of gas disappears. Due to very high local

supersaturations $S \sim 1000$ for both gases, the nanobubbles nucleate homogeneously nearby the electrodes. Nucleation happens in less than $10 \mu\text{s}$ as was observed experimentally for pulses of single polarity.⁴

The gas that is not consumed in the reaction results in the modest pressure increase that is observed. Still the concentration n_g of the survived gas must be high enough to sustain the short-lived MBs. This concentration was measured in two different ways using identical samples with a flexible and with a stiff membrane. The latter sample was not etched from the back side, and its membrane was completely immobilized. For the first sample, the deflection of the membrane was measured with the vibrometer from the back side of the wafer as shown schematically in Fig. 4. The process was driven at $U = 10 \text{ V}$ and $f = 100 \text{ kHz}$ during $400 \mu\text{s}$. Pressure in the chamber is shown in panel (a). Small pressure fluctuations are developed at $t > 300 \mu\text{s}$, indicating the very beginning of the transition to formation of the short-lived bubbles. The gas that results in the deflection of the membrane has to be collected in NBs because no light scattering is observed. Then, the concentration of gas averaged over the chamber volume \bar{n}_g is estimated as

$$\bar{n}_g = \frac{P + P_\gamma}{kT} \left(\frac{\Delta V}{V_{ch}} \right) \approx 3.5 \times 10^{25} \text{ m}^{-3}. \quad (1)$$

Here $P_\gamma = 2\gamma/r$ is the Laplace pressure in a NB of radius r , $\Delta V \approx 0.45V_{ch}\Delta d/h \approx 4500 \mu\text{m}^3$ is the volume increase under the clamped square membrane⁷ with the maximal deflection $\Delta d = 1 \mu\text{m}$, and h is the chamber height. The estimate is given for $r = 85 \text{ nm}$ (see below).

Figure 4(b) shows the evolution of the local gas concentration in the center of the chamber with a stiff membrane. The vibrometer was used to measure the change in the optical path caused by the gas present in the liquid.³ The diagram above panel (b) shows the measurement. Three main sources can contribute to the signal: change of the refractive index of the electrolyte due to presence of gas in any nonscattering form (dissolved gas or nanobubbles), change of the refractive index due to the temperature variation, and change due to the pressure variation in the chamber. The temperature increase

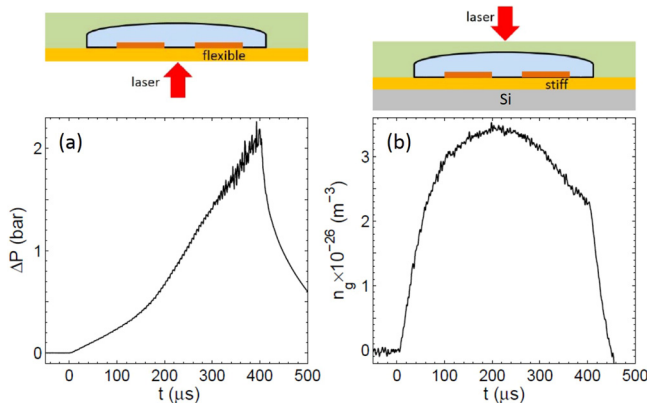


FIG. 4. (a) Overpressure in the chamber with a flexible membrane as measured with the vibrometer. The laser beam is reflected from the membrane. (b) Gas concentration in the center of the chamber with a stiff membrane. The laser beam passes through the liquid enriched with gas. The direction of the laser is shown in the diagram.

for this sample was estimated from the current as 5°C , which is much smaller than that for the sample with the flexible membrane ($40 - 50^\circ\text{C}$) due to a significant difference in thermal masses. The thermal effect can be responsible for 10% of the observed signal. The overpressure, $\Delta P \approx 6 \text{ bar}$, was estimated from the observation of a pinned bubble, which shrinks when the driving pulses are switched on. This pressure is larger than for the case of flexible membrane, but its contribution to the observed signal is about 3%. Therefore, the main contribution to the signal comes from the dissolved gas.

The gas concentration is significant only in between the electrodes and is maximal in the center of the chamber. Local concentration as high as $n_g = 3 \times 10^{26} \text{ m}^{-3}$ is observed. It is in a reasonable agreement with \bar{n}_g if we take into account that the gas is concentrated in between the electrodes. If all of this gas existed in the form of dissolved molecules, Henry's law would predict extremely high pressure $P \approx 560 \text{ bar}$. Energetically, it is more favorable for gas molecules to form bubbles than to stay squeezed in between the liquid molecules.⁸ The nonequilibrium state cannot exist longer than $10 \mu\text{s}$ (Ref. 4) before the bubble nucleation. Absence of a strong scattering signal at $\lambda = 633 \text{ nm}$ means that most of the gas is collected in NBs with the size $< \lambda/\pi$.⁹ In these small bubbles, the gas pressure is effectively shielded by the surface tension as described by Eq. (1). Normally, a separate NB would dissolve¹⁰ faster than the observation time in our experiments. However, in a closed container filled with gas-saturated liquid,^{8,11} NBs can survive much longer due to a collective effect known as “traffic jam” effect.

Our observations can be described by the following sequence of events. (i) Water electrolysis driven by alternating polarity voltage produces NBs containing either H_2 , O_2 , or a mixture of gases. The NBs containing a stoichiometric mixture disappear very fast due to spontaneous reaction.³ (ii) The bubbles containing mainly hydrogen or oxygen are collected in the chamber resulting in a steady pressure increase.⁵ (iii) When the density of NBs becomes so high that they touch, the bubbles merge and form a MB containing a stoichiometric mixture of H_2 and O_2 . (iv) In some way, this MB ignites spontaneously, resulting in an explosive pressure jump in the chamber. We discuss the steps (iii) and (iv) in more detail.

With the increases in gas concentration the density of NBs becomes so large that the bubbles will touch and coalesce. We can estimate the radii r of the NBs at this moment by requiring that the Laplace pressure $P_\gamma = 2\gamma/r$ inside them is high enough to store the measured concentration $n_{max} \approx 3 \times 10^{26} \text{ m}^{-3}$, and that these bubbles are closely packed. This gives $r \approx 2f_{cp}\gamma/n_{max}kT \approx 85 \text{ nm}$, where $f_{cp} \approx 0.74$ is the close-packing fraction of spheres.

The time scale τ_{col} for coalescence of two bubbles is given by a balance of viscous and capillary effects, resulting in $\tau_{col} = 4\pi r\eta/\gamma \sim 10 \text{ ns}$,¹² where $\eta \sim 10^{-3} \text{ Pa s}$ is the viscosity of the electrolyte. Therefore, if the density of NBs reaches the critical value, we expect the MB to appear very fast. A similar process was observed when a thin layer of liquid was superheated in a very short time.^{6,13-15} In this case, the coalescence of homogeneously nucleated vapor

bubbles led to the rapid formation of a macroscopic vapor film.

The fact that a single MB can lead to a considerable pressure increase in the much larger chamber, meaning that this is a highly energetic event. This amount of energy can appear only as a result of the reaction between H_2 and O_2 . The energy released in this reaction is $\delta E_{comb} = 2N|\Delta H|/3$, where $\Delta H \simeq -242$ kJ/mol is the enthalpy of water formation and N is the number of molecules in the MB after the coalescence of NBs. The bubbles we observe are flat bubbles with a height of $5 \mu\text{m}$ and radius $R = 3 - 5 \mu\text{m}$. The number of molecules in such a bubble at $P = 1.8$ bar and $T = 70^\circ\text{C}$ is estimated as $N = (0.5 - 1.5) \times 10^{10}$, and the combustion energy is in the range $\delta E_{comb} = 1.5 - 4$ nJ.

The energy needed to increase pressure in the chamber on $\delta P = 0.2$ bar is estimated as $\delta E_{ch} = \delta PV_{ch} \approx 1$ nJ. The reaction produces energetic molecules and radicals, which are able to vaporize water molecules from the bubble surface. This process can consume the rest of the combustion energy because the heat of vaporization $\Delta H_v = 41$ kJ/mol is significant. The other channels such as elastic energy of the membrane or kinetic energy of liquid play minor role in the energy balance.

In contrast with the standard combustion theory^{16,17} the temperature in MB cannot be significantly larger than the surrounding temperature. A characteristic time τ_h for the heat escape from a bubble of radius $R = 5 \mu\text{m}$ is estimated as $\tau_h \approx R^2/\pi^2\chi_g \sim 30$ ns, where $\chi_g \approx 0.9 \times 10^{-4} \text{ m}^2/\text{s}$ is the heat diffusion coefficient in the gas mixture. This is much faster than duration of the pressure jumps. This suggests that the reaction in micro and nanobubbles has to be a surface dominated process similar to the catalytic effect. Measurements with a low-light Andor iXon +855 EMCCD camera indicate the absence of any localized high temperature regions.

If the heating of the gas volume does not play a role, then the bubble's surface must be involved in the ignition of the reaction. The time scale for the reaction in this case will be given by the time for a gas molecule to diffuse to the bubble surface, $\tau_{react} \sim R^2/D_{gg} \sim 1 \mu\text{s}$, where $D_{gg} \approx 3.8 \times 10^{-5} \text{ m}^2/\text{s}$ is the diffusion coefficient in the stoichiometric mixture of gases at $P = 1.8$ bar.

In conclusion: By optical means, we observed microbubbles with a size of $\sim 10 \mu\text{m}$ which appear in a closed chamber just for a few microseconds as the result of the alternating polarity electrochemical process. Each event is accompanied by the energy release larger than 1 nJ. All the signatures of the process indicate that we observe combustion of hydrogen and oxygen in microbubbles.

We thank M. Elwenspoek, G. Krijnen, N. Tas, D. Lohse, S. Wildeman, M. V. Lokhanin, and V. V. Naumov for helpful discussions and R. Sanders for technical assistance. This work is supported by the Russian Science Foundation, Grant No. 15-19-20003. V.B.S. acknowledges partial support from the Netherlands Center for Multiscale Catalytic Energy Conversion (MCEC), and NWO Gravitation programme funded by the Ministry of Education, Culture and Science of the government of the Netherlands.

¹G. Vesper, *Chem. Eng. Sci.* **56**, 1265 (2001).

²A. C. Fernandez-Pello, *Proc. Combust. Inst.* **29**, 883 (2002).

³V. B. Svetovoy, R. G. P. Sanders, T. S. J. Lammerink, and M. C. Elwenspoek, *Phys. Rev. E* **84**, 035302(R) (2011).

⁴V. B. Svetovoy, R. G. P. Sanders, and M. C. Elwenspoek, *J. Phys.: Condens. Matter* **25**, 184002 (2013).

⁵V. B. Svetovoy, R. G. P. Sanders, K. Ma, and M. C. Elwenspoek, *Sci. Rep.* **4**, 4296 (2014).

⁶D. M. van den Broek and M. Elwenspoek, *J. Micromech. Microeng.* **18**, 064003 (2008).

⁷D. Maier-Schneider, J. Maibach, and E. Obermeier, *J. Microelectromech. Syst.* **4**, 238 (1995).

⁸J. H. Weijjs, J. R. T. Seddon, and D. Lohse, *Chem. Phys. Chem.* **13**, 2197 (2012).

⁹C. F. Bohren and D. Huffman, *Absorption and Scattering of Light by Small Particles* (John Wiley, New York, 1983).

¹⁰P. S. Epstein and M. S. Plesset, *J. Chem. Phys.* **18**, 1505 (1950).

¹¹J. H. Weijjs and D. Lohse, *Phys. Rev. Lett.* **110**, 054501 (2013).

¹²A. Eddi, K. G. Winkels, and J. H. Snoeijer, *Phys. Fluids* **25**, 13102 (2013).

¹³Z. Yin, A. Prosperetti, and J. Kim, *Int. J. Heat Mass Transfer* **47**, 1053 (2004).

¹⁴K. Okuyama, S. Mori, K. Sawa, and Y. Iida, *Int. J. Heat Mass Transfer* **49**, 2771 (2006).

¹⁵M. N. Hasan, M. Monde, and Y. Mitsutake, *Int. J. Heat Mass Transfer* **54**, 2844 (2011).

¹⁶B. Lewis and G. von Elbe, *Combustion, Flames and Explosions of Gases* (Academic Press, New York, 1987).

¹⁷G. W. Koroll, R. K. Kumar, and E. M. Bowles, *Combust. Flame* **94**, 330 (1993).